# Facilitating Interskin Communication in Artificial Polymer Systems through Liquid Transfer

ADVANCED MATERIALS
www.advmat.de

# Facilitating Interskin Communication in Artificial Polymer Systems through Liquid Transfer

*Dongyu Zhang, Dirk J. Broer, and Danqing Liu**

**Chemical communication is a ubiquitous process in nature, and it has sparked interest in the development of electric-sense-based robotic perception systems with chemical components. Here, a novel liquid crystal polymer is introduced that combines the transferring, receiving, and sensing of chemical signals, providing a new principle to achieve chemical communication in robotic systems. This approach allows for the transfer of cargo between two polymer coatings, and the transfer can be monitored through an electrical signal. Additionally, cascade transfer can be achieved through this approach, as the transfer of cargo is not limited to only two coatings, but can continue from the second to a third coating. Furthermore, the two coatings can be infused with different reagents, and upon exchange, a reaction takes place to generate the desired species. The novel method of chemical communication that is developed presents a notable improvement in embodied perception. This advancement facilitates human–robot and robot–robot interactions and enhances the ability of robots to efficiently and accurately perform complex tasks in their environment.**

## 1. Introduction

Chemical communication between individuals is a complex and dynamic process that involves the production, release, and recognition of chemical signals.[1] In many cases, chemical signals are used by organisms to communicate information about their identity, location, reproductive status, or physiological states.[2] For example, plants use chemical signals to attract pollinators or repel herbivores, while insects use pheromones to locate mates or mark their territory. In recent years, there has been growing interest in the use of chemical communication principles in the development of artificial systems, such as sensors, robots, and communication networks.[3] The ability to mimic and harness the power of chemical communication has the potential to revolutionize many aspects of modern technologies, from manufacturing and transportation to healthcare and exploration.

One key challenge in the development of chemical communication robotic systems is to enable them to perceive and interact with their environment in a way that is robust, adaptable, and ingenious. Inspired by the complex sensory abilities of living organisms, researchers have been exploring various ways to incorporate communication principles into robotic systems.[4] A promising approach is introducing electric-sense-based perception, which endows robots with the ability to detect and respond to electric charges in their environment. However, relying only on electric sensing is still not sufficient to manage the interaction between robots. The additional necessity is to control chemical release, thereby governing the emission of signals and ensuring a more comprehensive approach to robotic interaction.[5] Here in this work, we developed an artificial photoresponsive skin based on liquid crystal polymer networks (LCNs) that enables the controllable release, transfer, and sensing of chemical signals. The signal chemical was preloaded in the artificial skin as cargo, which can be released by triggering the deformation of the skin with light illumination. Besides, an inherent sensor was built up in the skin for the perception of environmental signals. Upon receiving chemicals from other skins, the skin as a receiver can exhibit both a visible transmittance change and a detectable electric signal change. Our approach to facilitating chemical communication between artificial polymer skins by triggered processes goes beyond the mere transfer of chemicals between two coatings. Instead, we achieve multiple transfers among coatings through diverse routes, taking this approach to a more advanced level. Additionally, the cargos in each two coatings can be different reagents. Upon a cargo transfer, a reaction takes place to generate the desired species. This feature greatly enhances the sophistication and nuance of electric-sense-based embodied robotic perception systems, paving the way for new possibilities in robotic control and interaction.

D. Zhang, D. J. Broer, D. Liu
Department of Chemical Engineering and Chemistry
Eindhoven University of Technology
Groene Loper 3, Eindhoven 5612 AE, The Netherlands
E-mail: d.liu1@tue.nl

D. Zhang, D. J. Broer, D. Liu
Institute for Complex Molecular Systems (ICMS)
Eindhoven University of Technology
Groene Loper 3, Eindhoven 5612 AE, The Netherlands

The ORCID identification number(s) for the author(s) of this article can be found under https://doi.org/10.1002/adma.202312428



**DOI: 10.1002/adma.202312428**

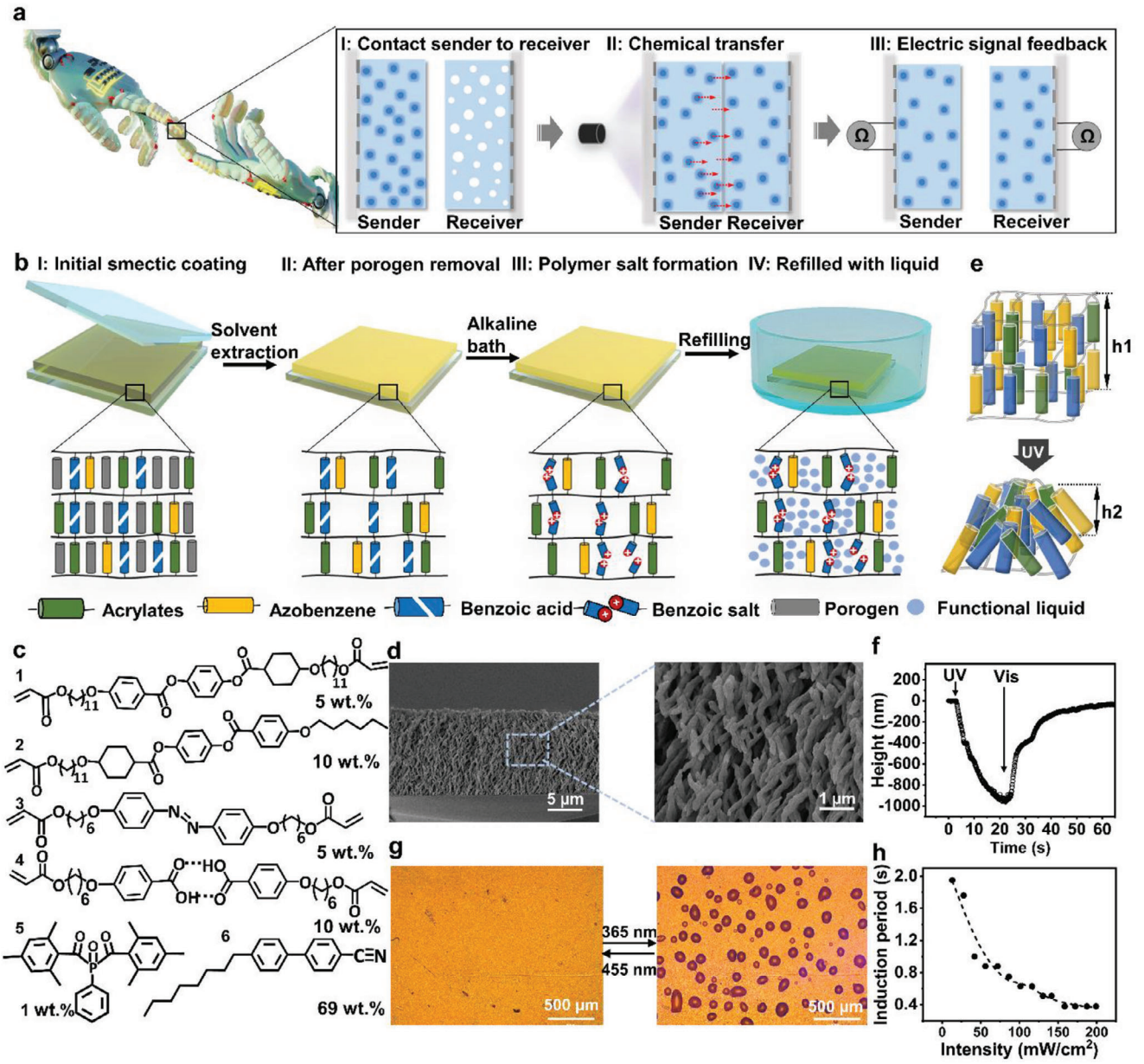


**Figure 1.** Design concept of LCN polymer coatings communicating for information transfer. a) Schematic illustration of the process of chemical communication, including information transfer, reception, and sensing. b) Fabrication procedure of the LCN coating on a glass substrate. c) Material composition of the communicating coating. (**1**, **2** LC monomers, **3** photoresponsive constituent, **4** benzoic acid dimer, **5** photoinitiator, **6** porogen). d) Cross-sectional scanning electron microscope (SEM) image of the porous LCN coating and its zoomed-in view of the SEM image in highlighting the porous structure. e) Scheme illustrating the smectic LC network and its contraction due to order decrease ($h2 < h1$). f) Coating surface height changes over time upon UV and visible light irradiation. g) Optical microscope images showing the secretion and reabsorption of PEG solution under light illumination at different wavelengths. h) Induction period of secretion upon UV illumination as a function of illuminating intensity.

## 2. Results and Discussion

The designed process of the chemical communication is shown in **Figure** 1a. To load our polymer skin with the desired chemicals, we infuse liquid with the desired chemicals (typically ionic species) into the porous matrix of the skin, which allows the skin to transfer chemical information to a second skin. In this case, a hand-over principle is employed, whereby the receiving skin is initially empty and can spontaneously accept the substance that is released on command from the first skin (sender). This transfer can be eventually detected by an electrical signal of the cargo to electrodes in the receiving layer. The material design concept of our smart skin is based on employing a LCN[5a,6] with homeotropic smectic order (Figure 1b,c). The smectic phase has a strong tendency to organize in layers with the molecular orientation (director) perpendicular to the layer as driven by surface tension. To make the artificial skin, a photoresponsive porous coating is obtained by blending the smectic

reactive monomers (molecules **1** and **2**), in the presence of a small amount of the azobenzene monomer (molecule **3**), with a smectic porogen (molecule **6**, 4′-Octyl-4-biphenylcarbonitrile, 8CB). As soon as the network is formed by photopolymerization, the non-reactive 8CB phase separates from the polymer network.[7] After removing the porogen, we obtain a LCN coating that contains nanometer to micrometer sized anisotropic pores (Figure 1d). By using monomers **1** and **2** alone, the polymer network is less compatible with high polar liquid compared to the one typically found in the majority of biological systems. To optimize this, we copolymerized a benzoic acid derivative (molecule **4**)[8] into our mixture. This derivative assembles into hydrogen-bridged dimer which has liquid crystal properties and preserves the smectic phase of monomers **1** and **2**. Following the photo-cross-linking and the removal of porogen, the coating is then exposed to a basic solution where the benzoic acid dimers undergo an ionic state transition, thus changing the LCN coating from hydrophobic to hydrophilic (Figure 1b,c and Figure S1 (Supporting Information)). The obtained porous LCN coating can be saturated with some polar liquid, thereby loading it with cargos that can be subsequently released upon actuation. Optically, the initial coating is transparent when the porogen is still inside, but changes into opaque after extracting the porogen (Figures S2 and S3, Supporting Information), primarily due to the refractive index mismatch between the air trapped within the voids and the solid polymer matrix.[9] Upon loading empty pores with the desired polar liquid, such as ethylene glycol (EG) or polyethylene glycol (PEG), its transparency increases again (Figure S4, Supporting Information). To facilitate electrical sensing upon transfer of the liquid, a small trace of NaCl was dissolved in the liquid and infused into the coating with the liquid. In this way, an ionic-solution-filled LCN coating is prepared to function as the information-transferring sender. The same coating, yet unfilled, can also serve as a receiver of liquid. Typically, the thickness of both the sender and the receiver coating is designed to be 20 µm, which does not change obviously no matter if the coating is filled or empty (Figure 1d).

The principle to make the sender release chemical information is based on the UV-light-promoted *trans*-to-*cis* isomerization of the copolymerized azobenzene moieties.[10] This results in a decrease in the scalar order and a corresponding contraction of the film. Specifically, LCNs contract along the direction of molecular alignment and expand in two perpendicular directions when order decreases.[11] In a coating configuration, the in-plane expansion is restricted due to strong adhesion to the rigid substrate. Consequently, the homeotropically aligned polymer coating undergoes a 5% reduction in thickness (as shown in Figure 1e,f), causing the pores to shrink and exert pressure on the liquid, thereby expelling the liquid at the coating surface (Figure 1g and Movie S1 (Supporting Information)). The time scale of this secreting process can be fine-tuned by varying the intensity of the light source (Figure 1h).[12]

To initiate the transfer of chemical information, we bring the sender and receiver into close contact. The transfer process is illustrated in **Figure 2**a. UV light is employed to stimulate the release of chemicals from the sender. We have optimized the thickness of the sender component in order to prevent UV light from permeating through the sender to the receiver, thus avoiding unwanted actuation and secretion by the receiver. The UV–vis spectrum analysis confirms that minimal UV light has penetrated through the sender, even when taking into account the photobleaching azobenzene during its *trans*-to-*cis* conversion (Figure S5, Supporting Information). Then, we monitor the liquid transfer process by observing the interface between the sender and the receiver under an optical microscope in transmission mode (Figure 2b–d and Movie S2 (Supporting Information)). Initially, before the liquid transfer, the view appears black due to light scattering by the empty receiver. However, during the liquid transfer, bright regions emerge, indicating the absorption of the liquid by the receiver. Eventually, the entire view becomes bright, signifying the complete filling of the coating. Macroscopically, the liquid acceptance is also visible because the receiver changes from opaque to transparent upon receiving liquid (Figure 2e–g). This receiving process is facilitated by the capillary force and interfacial interactions between the liquid and network phases, as indicated by the liquid equilibrium contact angle, $\theta_{eq}$.[13] According to the Washburn equation,[14] the liquid absorption height $h$ within a horizontal capillary is related to the contact angle: $h^2 = \frac{r\gamma \cos\theta}{2\eta} t$, where $r$ is the radius of the capillary; $\gamma$ and $\eta$ are the surface tension and viscosity of the liquid; $\theta$ is the contact angle and $t$ is the time of duration of the diffusion process. In a porous structure, the spontaneous imbibition behaves as an assemblage of very small cylindrical capillaries. When $0 < \theta_{eq} < \theta_c < \pi/2$ ($\theta_c$ depends on the roughness and characteristics of the porous structure), the liquid can be continuously imbibed into the pores.[15] Here, by tuning the surface tension of the infused liquid or the polarity of our coating, we can reduce $\theta_{eq}$ to an appropriate value, therefore enhancing the imbibition capability (Figure S6, Supporting Information).

The receiver coating is applied on a substrate with an interdigitated electrode (IDE) array which senses the quantity of the transferred liquid via an electrical signal change (**Figure 3**a). We measure the dynamic resistance of the receiver during liquid transfer. As shown in Figure 3b, by illuminating the sender with 200 mW $cm^{-2}$ UV light as an optical input, the resistance instantly decreases from infinity to ≈20 MΩ. We establish a correlation between resistance and liquid quantity of the receiver, which is further fitted by a reciprocal function given the multiparallel circuit structure of the IDE array (Figure 3c–e). The reliability of this measurement is demonstrated by consistent data obtained across three repetitive cycles. In this way, we estimate that 0.93 mg of ionic solution has been transferred to the receiver within 200 s of UV illumination, which is equal to 51.1 wt% of total liquid in the sender (Figure 3d). Interestingly, according to the coating's deformation, the sender usually secretes 5% of the liquid in the absence of the receiver, with additional secretion occurring upon contact with an empty receiver. To visualize the chemical information transfer, we established a series connection by linking the IDE of the receiver with both a light-emitting diode (LED) bulb and a direct current power supply (Figure 3f,g). Upon receiving the liquid, the receiver with decreased resistance facilitates the flow of current in the circuit, thereby initiating the LED bulb to emit light (Figure 3h and Movie S3 (Supporting Information)).

In order to expand on the versatility of the system, we explore the possibility of using the receiver to operate as a sender and return the liquid back to the initial sender. To achieve a higher transfer efficiency, here the coatings are filled with ionic EG solution due to its lower viscosity and better mobility. Already in

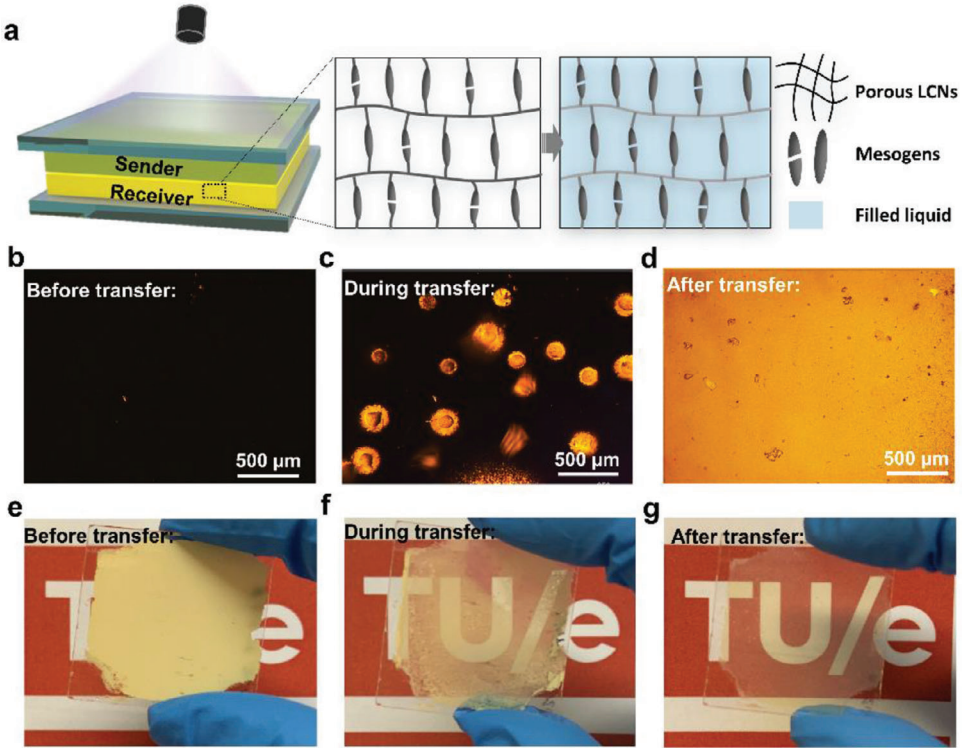


**Figure 2.** Visual feedback of liquid transfer from sender to receiver coating. a) Scheme illustrating the receiver being infused with liquid upon liquid transfer from the sender. Here the liquid preloaded to the sender is a PEG solution. Optical microscope images showing the interface of the receiver and sender b) before, c) during, and d) after liquid transfer. Photograph images of the receiver, with a TU/e logo background, showing the change in transparency with e) empty receiver before liquid transfer and the filled receiver f) during, and g) after the liquid transfer (for an adequate liquid infusion, the receiver demonstrated in this case has a thickness of 6 μm).

the first experiment (as shown in **Figure** 4a,d,e), we demonstrate that by now exposing the film at the receiver side (coating B), 37.7 wt% of the liquid could be sent back to the initial sender (coating A). Then, we replenish the sender A with enough ionic EG to initiate a new round of transfers. We found that the sender can transfer its liquid to multiple empty receivers. As shown in Figure 4b,d,f, initially sender A transfers 60.3 wt% of its liquid to receiver B. In a subsequent transfer, another 19.3 wt% of the initial liquid amount is delivered from sender A to the second receiver B1. However, when attempting to transfer to the third receiver, B2, further liquid transfer is hampered within the time scale of the experiment, resulting in 20.4 wt% of the liquid remaining in sender A. Apparently, the remaining EG has a strong interaction with the liquid crystal network and cannot be photomechanically removed. Besides the given properties, a cascade transfer (Figure 4c,d,g,h) can be performed among several empty coatings, wherein the receiver B can further transfer 47.2 wt% of received liquid to another empty receiver C, and then extend the transfer to more empty receivers. This iterative process can be repeated for four consecutive transfers, culminating in the final receiver being infused with 0.11 mg liquid, corresponding to 7.3 wt% quantity of initial liquid.

Next, we advance the developed information transfer system with different reagents. Upon exchange, a reaction takes place to generate the desired species. In this experiment, the sender is loaded with potassium thiocyanate (KSCN) dissolved in PEG, while the receiver is loaded with ferric chloride dissolved in PEG. These specific reagents are selected for their ability to generate a colored product, facilitating direct visual signaling. **Figure** 5a,b clearly shows that upon exposure to UV light illumination, an intense red color is produced within seconds. During this process, the sender transfers its KSCN to the receiver. Subsequently, the ferric ions ($Fe^{3+}$) present in the receiver form a charge transfer complex with the thiocyanate ions ($SCN^-$), leading to a reaction that produces the red-colored product, as is also shown in Movie S4 (Supporting Information).

Because the transfer process is initiated by light, it can in principle be done pattern-wise by local exposure. An issue to solve is the capillary wetting of the whole sender/receiver interface as soon as the messenger liquid is released from the sender. To enhance the resolution and confine the reaction to a specific area, we establish a distance between the sender and the receiver to prevent the excreted droplets from coming into direct contact with the receiver and spreading across the plane. We have implemented a 10 μm gap between the sender and receiver, ensuring that it is greater than the height of all the droplets at the sender (Figure 5c). The liquid in the sender is replaced with an evaporable ionic EG solution. As depicted in Figure 5d,e, upon UV illumination, $2.92 \times 10^{-4}$ μL of the liquid is ejected from the sender and accumulates at the surface, forming droplets with heights mostly ranging from 3.5 to 6 μm with a maximum of 6.5 μm, as determined by a digital holographic microscope (DHM). These droplets are subsequently dispersed to the air, as indicated by a decrease in volume at the sender surface (Figure 5f and

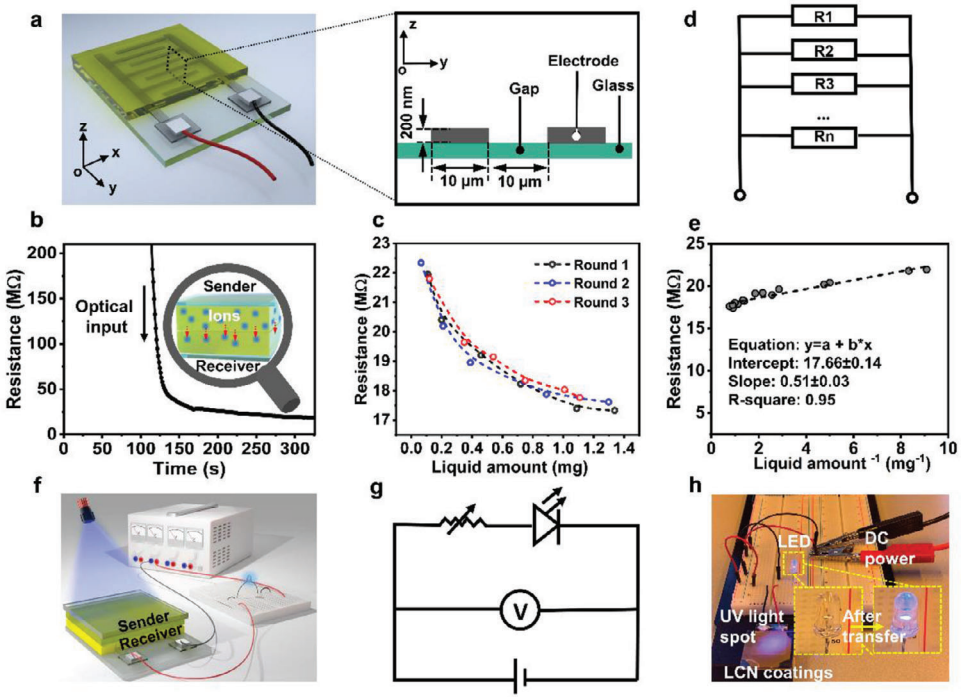


**Figure 3.** Chemical information transfer and sensing. a) The schematic diagram showcases the coating arrangement in both the sender and receiver, where the IDEs are topped with an azobenzene-containing LCN coating. A cross-sectional perspective of the IDEs reveals their structure, with each electrode measuring 10 μm in width and being separated by a 10 μm gap. b) Resistance change of the receiver upon activating the sender. c) The resistance of the receiver as a function of the amount of infused liquid. d) Equivalent electric circuit of the IDE. e) Utilizing the reciprocal function to fit the data from (c). f) Illustration of the device configuration for chemical information transfer. g) The equivalent electrical circuit corresponding to the system in (f). h) Experiment showing the LED illumination and the transfer of the ionic solution.

Figure S7 (Supporting Information)), possibly accelerated by the heat generated by the UV light (Figure S8, Supporting Information). Then, we introduce a photomask between the light source and the coatings, as shown in Figure 5g. Upon applying the optical input to the sender, the image information contained in the photomask is then imprinted onto the receiver (Figure 5g–j and Movie S5 (Supporting Information)). Although location-resolved proximity vapor transport of organic material is well accepted in literature, we were surprised about the accurate cotransfer of our inorganic ions with ethylene glycol. Actually, inorganic species transport over short distances is not uncommon in literature due to mechanical disturbance.[16] The imprinted image on the receiver can stay for more than 1 h, and it can be erased by water. By utilizing this distanced transfer method, it becomes possible to achieve a resolution of 500 um for the image imprinting (Figure S9, Supporting Information).

## 3. Conclusion

In conclusion, our liquid crystal polymer material facilitates the light-triggered transfer of chemical signals between layers of artificial polymer skin, enabling the sensing and responsiveness necessary to perceive and react to environmental cues. This breakthrough holds great potential for future research in the field of robotic sensory and feedback systems. Furthermore, the material's ability to facilitate chemical reactions between the polymer skins has significant implications for enabling complex interactions among surfaces of objects. By harnessing the capacity to initiate a series of chemical reactions using our material, multi-robot systems can collaborate effectively to achieve specific tasks. For example, robots equipped with our material can coordinate their actions to construct complex structures or carry out a series of predefined actions in response to external stimuli. Other than light responsiveness, electric-responsive liquid transfer is also achieved, which may boost the electrical signal control platform applied for this robot communication (Figure S11, Supporting Information). Overall, our work presents a promising approach to the development of communication materials that successfully emulate the complexity observed in biological sensory systems, thereby paving the way for new opportunities in robotic sensing and control. Future efforts will seek to explore multiple sensors embedded in the smart LCN coatings and their better adaption, making robotics more collaborative and effective in diverse complex scenarios.

## 4. Experimental Section

*Materials*: Diacrylate molecule **1** was purchased from Syncom B.V. Monoacrylate molecule **2**, azobenzene derivative **3**, and low-molecular-mass liquid crystal **6** (4′-Octyl-4-biphenylcarbonitrile, 8CB) were purchased from Synthon Chemicals. Benzoic acid molecule **4** (6OBA) was purchased from AmBeed. Molecule **5** (Irgacure 819) was purchased from Ciba. A typical recipe that was used in this work was a mixture that contained 5 wt% diacrylate **1**, 10 wt% monoacrylate **2**, 5 wt% azobenzene diacrylate **3**, 10 wt% benzoic acid molecule **4**, 69% nonreactive porogen

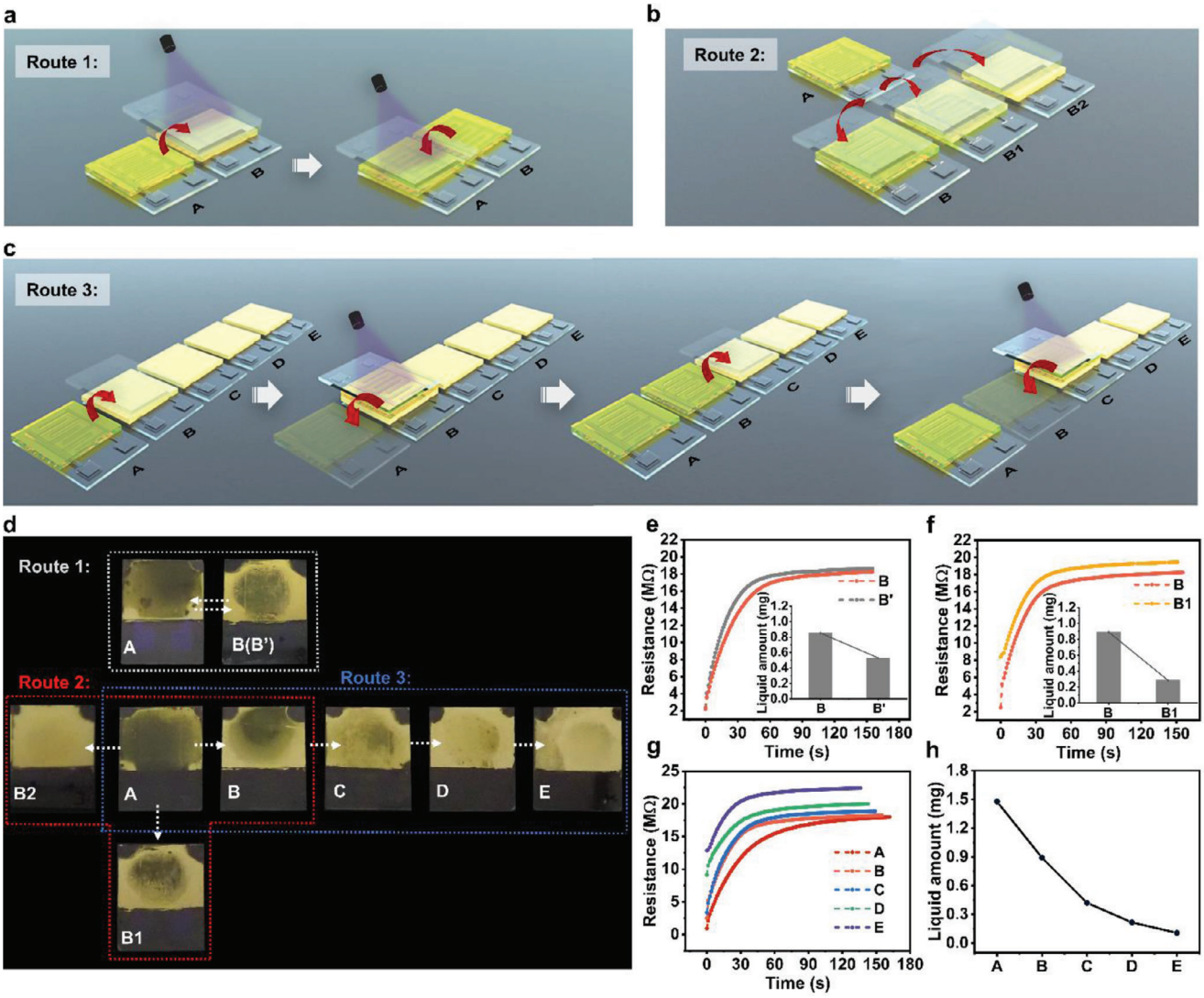


**Figure 4.** Sequential liquid transfer through diverse routes. Schematic illustration of a) Route 1, reciprocal liquid transfer, b) Route 2, distribution transfer, and c) Route 3, cascade transfer. d) Photographs of LC coatings demonstrating three distinct pathways for the transfer of liquid sequentially. In Route 1, the liquid transferred to receiver B is returned to sender A. In Route 2, the liquid is distributed toward several empty receivers. Route 3 involves a cascade transfer of the liquid from coating A to coating E. e) The electric signal of receiver B after receiving liquid from sender A (noted as B) and after sending liquid back to sender A (noted as B′) through Route 1. f) The electric signal of receiver B and B1 after sequentially receiving liquid from sender A through Route 2. The resistance of receiver B2 is too high to be measured. Insets are the evaluated amount of liquid in the coatings according to their resistance. g) The electric signal of coating A to E through cascade transfer in Route 3 and h) the corresponding liquid amount in each coating.

**6**, and 1.0 wt% photoinitiator **5**. For control experiments, the amount of benzoic acid molecule **4** was varied between 0, 5, 15, and 20 wt%, respectively. All the liquid crystal monomer mixtures were made by dissolving them in dichloromethane and then evaporating the solvent at 70 °C. Ethylene glycol (Sigma-Aldrich) and polyethylene glycol 200 ($M_n$ = 190–210 g mol$^{-1}$) (Sigma-Aldrich) were used as received. Potassium hydroxide (Sigma-Aldrich) solution (0.5 M) was prepared by dissolving solid material in distilled water. Sodium chloride (Sigma-Aldrich) solution (0.1 M), iron(III) chloride (Sigma-Aldrich) solution (1 M), and potassium thiocyanate (Sigma-Aldrich) solution (1 M) were prepared by dissolving solid materials in distilled water and polyethylene glycol (or ethylene glycol in some cases) (1:24 in volume). Glass substrates with interdigitated indium tin oxide electrodes (active area: 1.4 × 1.0 cm) were purchased from Walthy Precision Co., Ltd.

*Sample Preparation*: LCN coatings with homeotropic alignment were fabricated by photopolymerizing the liquid crystal monomer mixture in a cell at 34 °C (unless otherwise specified, the thickness of coating was fixed at 20 μm). The cells were formed by gluing two glass substrates with a gap of 20 μm as confined by spherical beads (Sekisui Chemical Co., Ltd.). In particular, one of the glass substrates was precoated with polyimide layer (SE 5661, Nissan Chemicals) for homeotropic alignment. The other IDE substrate was precoated with 3-(trimethoxysilyl) propyl methacrylate (Sigma-Aldrich) to anchor the LCN coating. The liquid crystal monomer mixture was filled in the cell by capillary force in its isotropic phase and then cooled down to smectic phase. Next, the mixture was polymerized by a UV lamp (Omnicure EXFO S2000). A cutoff filter (Newport FSQ-GG400 filter) between the lamp and the sample blocked the light <400 nm to prevent premature isomerization of azobenzene. After photopolymerization,

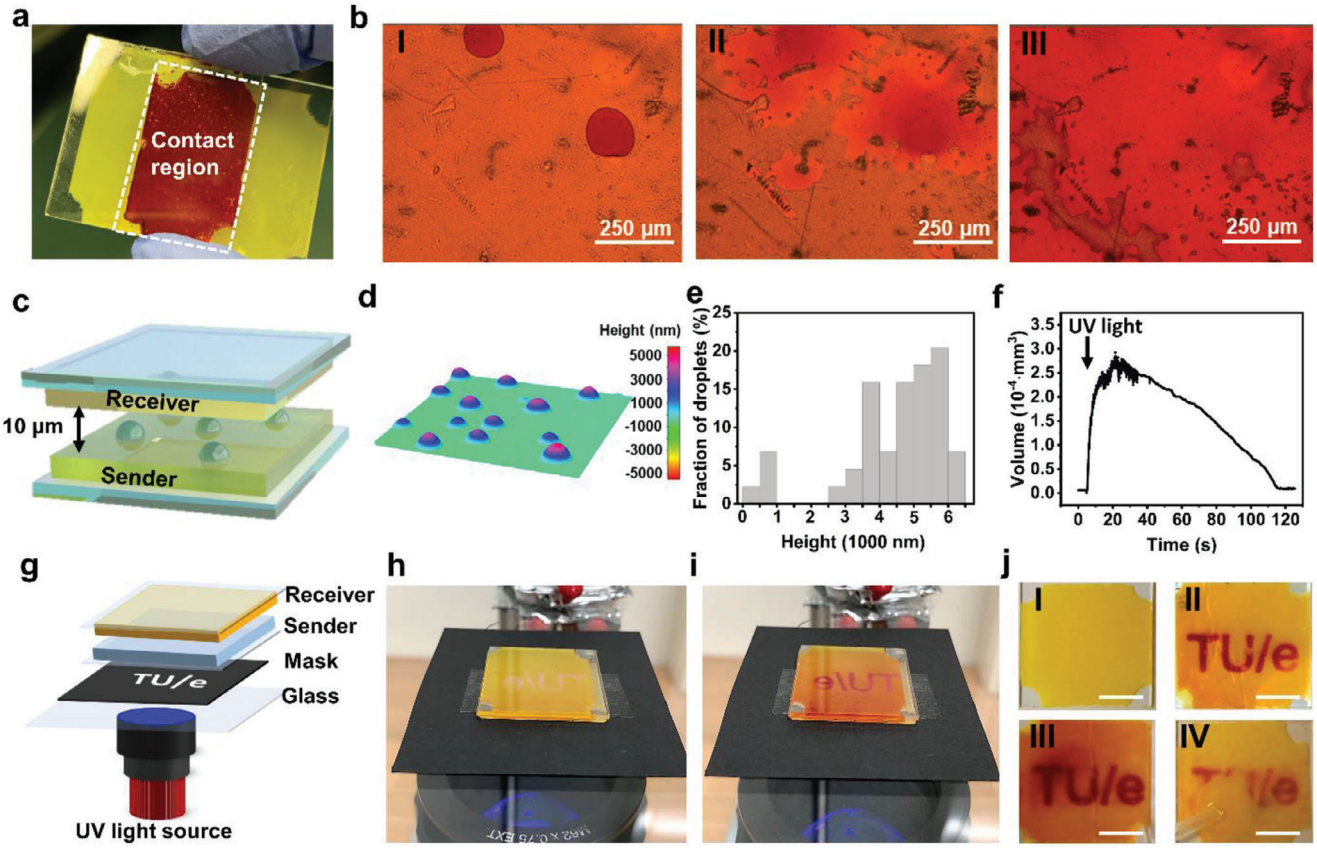


**Figure 5.** Chemical communication facilitates chemical reactions. a) The photograph captures a chemical reaction spread across the entire surface, with b) zoomed microscopic images revealing the distribution of the formed $Fe(SCN)_3$ throughout the surface (I: 7 s, II: 11 s, and III: 34 s after UV illuminating). c) Schematic illustration of vapor transfer over a distance of 10 μm. d) A DHM image illustrates the secreted KSCN solution droplets formed on coating surface. e) The distribution of droplet heights depicted from 3 times DHM measurements. f) Changes in the volume of KSCN droplets at the coating surface upon UV illumination. g) A 3D illustration showcases the localized vapor transfer, along with h–j) the corresponding experimental results. Optical photographs showing the (h) initial receiver before KSCN solution transfer and (i) the red patterns appear on the receiver after KSCN transfer. (j) The photographs in top view showing the receiver I) before KSCN transfer, II) after KSCN transfer, III) being kept after chemical transfer for 1 h, and IV) being washed with water to remove the resultant pattern.

the glass substrate with a polyimide alignment layer was removed. The polymerized coating at the other glass substrate was immersed in 200 mL cyclohexane for 24 h to wash out the porogen. Then, an alkaline bath to the porous coating was performed using 0.5 M KOH solution to break the hydrogen bonds between the carboxylic acid groups. After that, the LCN coating could be filled with the desired liquid by absorbing the liquid into the pores via capillary force (azobenzene in the network should be kept in a *trans*-state).

*Characterization*: The alignment and optical property of LCN coating were observed by a cross-polarized optical microscope (Leica DM2700). Phase-transition temperatures of liquid crystal monomer mixtures were measured by Differential scanning calorimetry (Q2000, TA Instruments) at a rate of 10 °C $min^{-1}$. The thickness and surface profile of samples were measured by interferometer (Sensofar S neox). The liquid secreted on the surface of the LCN coating was quantified by a DHM (DHM-R and DHM-T, Lyncée Tec.) combined with image analysis. The microstructure of the LCN coating was observed with a scanning electron microscope (FEI SEM Quanta 3D FEG) in secondary electron mode. The transmission of the LCN coating was measured by a spectrophotometer (PerkinElmer LAMBDA 750 UV/vis/NIR spectrophotometer). The temperature increase of the coating during UV illumination was monitored by infrared thermometers (Fluke Ti32 thermal imager). The weight of the liquid amount in the LCN coating was measured by Electronic Balance (Sartorius Micro MC 210 P). To keep the distance between the sender and receiver for chemical transfer, spherical beads (Sekisui Chemical Co., Ltd.) with a diameter of 10 μm were placed at the interface of two coatings.

To quantify the amount of liquid infused into the receiver, the resistance of the receiver coating was measured using a SourceMeter (Keithley 2400). Initially, the resistance of the coating was measured when it was filled with a liquid of known weight, and the resulting resistance after equilibrium was recorded as the dependent variable. Subsequently, the equilibrium resistance $R$ changes were plotted and fitted with the amount of liquid $w$ via reciprocal function $R = a + b \cdot w^{-1}$, where $a$ and $b$ were the intercept and slope, respectively. Using this fitted function, the quantity of received liquid was evaluated by applying its equilibrium resistance value. For the visualization of the liquid transfer via LED circuit, the circuit current was maintained by a direct current power supply (3B Scientific U33000). For the electric-responsive liquid transfer system, the alternating electric field with a sinusoidal wave function was provided by a function generator (Tektronix AFG3252C). The electric signal from the function generator was amplified by a high-voltage linear amplifier (Falco Systems WMA-300). The output voltage was measured by an oscilloscope (InfiniiVision DSO-X 3032T, Keysight).

## Supporting Information

Supporting Information is available from the Wiley Online Library or from the author.

## Acknowledgements

The authors thank Jacques Peixoto for doing the image analysis. The authors thank Tom Bus for taking SEM images. The authors thank Charlotte Bording for drawing the schematic illustration of the soft robot hands. D.Z. was financially supported by the China Scholarship Council (CSC). Funding: this research formed part of the research program financed by the Dutch Research Council (NWO) (OCENW.KLEIN. 10854, START-UP 8872, and Gravity Program 024.005.020 – Interactive Polymer Materials IPM).

## Conflict of Interest

The authors declare no conflict of interest.

## Author Contributions

D.J.B. and D.L. conceived the research and supervised the project. D.Z. performed experiments, analyzed the data, and drafted the paper. D.Z., D.J.B., and D.L. wrote the paper.

## Data Availability Statement

The data that support the findings of this study are available from the corresponding author upon reasonable request.

## Keywords

chemical communication, electric-sense-based perception, liquid crystal networks, responsive polymer materials

Received: November 20, 2023
Revised: January 3, 2024
Published online: January 20, 2024

[1] A. Llopis-Lorente, P. Díez, A. Sánchez, M. D. Marcos, F. Sancenón, P. Martínez-Ruiz, R. Villalonga, R. Martínez-Máñez, *Nat. Commun.* **2017**, *8*, 15511.

[2] a) C. Carmona-Fontaine, H. K. Matthews, S. Kuriyama, M. Moreno, G. A. Dunn, M. Parsons, C. D. Stern, R. Mayor, *Nature* **2008**, *456*, 957; b) A. Shemi, U. Alcolombri, D. Schatz, V. Farstey, F. Vincent, R. Rotkopf, S. Ben-Dor, M. J. Frada, D. S. Tawfik, A. Vardi, *Nat. Microbiol.* **2021**, *6*, 1357; c) N. K. Björkström, B. Strunz, H.-G. Ljunggren, *Nat. Rev. Immunol.* **2022**, *22*, 112.

[3] a) C. Giménez, E. Climent, E. Aznar, R. Martínez-Máñez, F. Sancenón, M. D. Marcos, P. Amorós, K. Rurack, *Angew. Chem., Int. Ed. Engl.* **2014**, *53*, 12629; b) J. Li, W. D. Jamieson, P. Dimitriou, W. Xu, P. Rohde, B. Martinac, M. Baker, B. W. Drinkwater, O. K. Castell, D. A. Barrow, *Nat. Commun.* **2022**, *13*, 4125; c) A. Llopis-Lorente, P. Díez, A. Sánchez, M. D. Marcos, F. Sancenón, P. Martínez-Ruiz, R. Villalonga, R. Martínez-Máñez, *Nano Today* **2018**, *18*, 8; d) O. Rifaie-Graham, J. Yeow, A. Najer, R. Wang, R. Sun, K. Zhou, T. N. Dell, C. Adrianus, C. Thanapongpibul, M. Chami, S. Mann, J. R. de Alaniz, M. M. Stevens, *Nat. Chem.* **2023**, *15*, 110; e) M. Chen, S.-M. Lu, H.-W. Wang, Y.-T. Long, *Angew. Chem., Int. Ed. Engl.* **2023**, *62*, 202215631; f) C. Chen, X. Chang, H. Teymourian, D. E. Ramírez-Herrera, B. Esteban-Fernández de Ávila, X. Lu, J. Li, S. He, C. Fang, Y. Liang, F. Mou, J. Guan, J. Wang, *Angew. Chem., Int. Ed. Engl.* **2018**, *57*, 241; g) A. D. Pizarro, C. L. A. Berli, G. J. A. A. Soler-Illia, M. G. Bellino, *Nat. Commun.* **2022**, *13*, 3047; h) P. Remón, U. Pischel, *ChemPhysChem* **2017**, *18*, 1667.

[4] a) G. Villar, A. D. Graham, H. Bayley, *Science* **2013**, *340*, 48; b) H. Tian, C. Wang, Y. Chen, L. Zheng, H. Jing, L. Xu, X. Wang, Y. Liu, J. Hao, *Sci. Adv.* **2023**, *9*, eadd6950.

[5] a) A. H. Gelebart, D. Liu, D. J. Mulder, K. H. J. Leunissen, J. van Gerven, A. P. H. J. Schenning, D. J. Broer, *Adv. Funct. Mater.* **2018**, *28*, 1705942; b) Y. Zhan, G. Zhou, B. A. Lamers, F. L. Visschers, M. M. Hendrix, D. J. Broer, D. Liu, *Matter* **2020**, *3*, 782; c) Y. Xu, Y. Chang, Y. Yao, M. Zhang, R. L. Dupont, A. M. Rather, X. Bao, X. Wang, *Adv. Mater.* **2022**, *34*, 2108788.

[6] a) T. J. White, D. J. Broer, *Nat. Mater.* **2015**, *14*, 1087; b) F. Ge, Y. Zhao, *Adv. Funct. Mater.* **2020**, *30*, 1901890.

[7] a) J. Kim, P. Palffy-Muhoray, *Mol. Cryst. Liq. Cryst.* **1991**, *203*, 93; b) J. Y. Kim, C. H. Cho, P. Palffy-Muhoray, T. Kyu, *Phys. Rev. Lett.* **1993**, *71*, 2232.

[8] K. D. Harris, C. W. M. Bastiaansen, D. J. Broer, *J. Microelectromech. Syst.* **2007**, *16*, 480.

[9] a) X. Yao, Y. Hu, A. Grinthal, T.-S. Wong, L. Mahadevan, J. Aizenberg, *Nat. Mater.* **2013**, *12*, 529; b) Y. Li, Q. Fu, X. Yang, L. Berglund, *Philos. Trans. R. Soc., A* **2017**, *376*, 20170182.

[10] a) Y. Xu, A. M. Rather, Y. Yao, J.-C. Fang, R. S. Mamtani, R. K. A. Bennett, R. G. Atta, S. Adera, U. Tkalec, X. Wang, *Sci. Adv.* **2021**, *7*, eabi7607; b) A. M. Rather, Y. Xu, Y. Chang, R. L. Dupont, A. Borbora, U. I. Kara, J.-C. Fang, R. Mamtani, M. Zhang, Y. Yao, S. Adera, X. Bao, U. Manna, X. Wang, *Adv. Mater.* **2022**, *34*, 2110085; c) Y. Hao, S. Huang, Y. Guo, L. Zhou, H. Hao, C. J. Barrett, H. Yu, *J. Mater. Chem.* **2019**, *7*, 503; d) H. Yu, *Dancing with Light: Advances in Photofunctional Liquid-Crystalline Materials*, CRC Press, Boca Raton, FL, USA **2015**; e) K. Mukai, M. Hara, H. Yabu, S. Nagano, T. Seki, *Adv. Mater. Interfaces* **2021**, *8*, 2100891; f) K. Mukai, K. Imai, M. Hara, S. Nagano, T. Seki, *ChemPhotoChem* **2019**, *3*, 495.

[11] D. Liu, C. W. M. Bastiaansen, J. M. J. den Toonder, D. J. Broer, *Angew. Chem., Int. Ed. Engl.* **2012**, *51*, 892.

[12] T. Guo, A. Svanidze, X. Zheng, P. Palffy-Muhoray, *Appl. Sci.* **2022**, *12*, 7723.

[13] a) T.-S. Wong, S. H. Kang, S. K. Y. Tang, E. J. Smythe, B. D. Hatton, A. Grinthal, J. Aizenberg, *Nature* **2011**, *477*, 443; b) R. N. Wenzel, *Ind. Eng. Chem. Res.* **1936**, *28*, 988; c) S. Das, H. V. Patel, E. Milacic, N. G. Deen, J. A. M. Kuipers, *Phys. Fluids* **2018**, *30*, 012112.

[14] a) E. W. Washburn, *Phys. Rev.* **1921**, *17*, 273; b) J. Zhang, J. Tuohey, N. Amini, D. A. V. Morton, K. P. Hapgood, *Chem. Eng. Sci.* **2021**, *245*, 116967; c) Y. Cui, Y. Wang, Z. Shao, A. Mao, W. Gao, H. Bai, *Adv. Mater.* **2020**, *32*, 1908249.

[15] L. Courbin, E. Denieul, E. Dressaire, M. Roper, A. Ajdari, H. A. Stone, *Nat. Mater.* **2007**, *6*, 661.

[16] a) A. E. Williams-Jones, C. A. Heinrich, *Econ. Geol.* **2005**, *100*, 1287; b) P. Loche, D. J. Bonthuis, R. R. Netz, *Commun. Chem.* **2022**, *5*, 55; c) P. Jungwirth, D. J. Tobias, *Chem. Rev.* **2006**, *106*, 1259.